Letters

Elimination of Mutual Flux Effect on Rotor Position Estimation of Switched Reluctance Motor Drives Considering Magnetic Saturation

Jin Ye, *Student Member, IEEE*, Berker Bilgin, *Member, IEEE*, and Ali Emadi, *Fellow, IEEE*

***Abstract*—In this letter, an approach to eliminate the mutual flux effect on the rotor position estimation of switched reluctance motor drives without *a priori* knowledge of mutual flux is proposed, while operating in both linear and saturated magnetic regions. Considering magnetic saturation, the incremental-inductance estimation using the phase current slope difference method can be classified into three modes: Modes I–III. At positive-current-slope and negative-current-slope sampling point of one phase, the sign of current slope of the other phase changes in Modes I and II, but does not change in Mode III. Theoretically, the incremental-inductance estimation error introduced by the mutual flux is both rotor position and phase current dependent, which is ±1% to ±7% for the studied motor in Modes I and II. However, in Mode III, the mutual flux effect does not exist. Therefore, two methods are proposed to ensure that the incremental-inductance estimation is working in Mode III exclusively. The first one is variable-sampling incremental-inductance estimation for the outgoing phase and the other is the variable-hysteresis-band current control for the incoming phase. Simulation and experimental results show that the proposed method improves position estimation accuracy by 2° compared with the conventional method without variable-sampling and variable-hysteresis-band current control.**

***Index Terms*—Magnetic saturation, mutual flux, rotor position estimation, switched reluctance motor (SRM) drives.**

I. Introduction

POSITION sensorless control of a switched reluctance motor (SRM) is gaining interest in recent years in low-cost motor drives [1]–[10]. Most approaches are focused on estimating the flux linkage, inductance or electromagnetic force, which are rotor position dependent. The mutual flux effect has been widely included in equivalent circuit modeling of the SRM [11]–[13]; however, the mutual flux effect has not been fully considered in the rotor position estimation. In [14] and [15], the mutual flux effect on the flux linkage estimation of the SRM is studied and then the mutual flux is simulated or measured in advance to calibrate the estimated flux linkage. By considering the mutual flux, rotor position estimation accuracy is improved. However, the mutual flux simulation or measurement may not be accurate due to noise or manufacturing imperfections. Also, flux-linkage-based rotor position estimation methods suffer from the low accuracy at low speed. In [16], an approach to eliminate the mutual flux effect on the rotor position estimation is presented without *a priori* knowledge of mutual flux of SRM. Self-inductance is estimated by the current slope difference method and this method is capable of working at the wide speed range, but the operation is limited to linear magnetic region only.

In this letter, without dependence on mutual flux profiles, two methods are proposed to eliminate the mutual flux effect on the rotor position estimation of SRM drives working in both linear and magnetic saturation regions: 1) variable sampling for the outgoing-phase incremental-inductance estimation; and 2) variable-hysteresis-band current control for the incoming-phase incremental-inductance estimation. Considering the mutual coupling and magnetic saturation, instead of self-inductance, the incremental inductance is estimated, by using the phase current slope difference method. Then, theoretical analysis of the incremental-inductance estimation error introduced by the mutual flux is provided. Three operational modes are defined for incremental-inductance estimation. In Modes I and II, at the positive-current-slope and negative-current slope sampling point of one phase, the sign of the current slope of the other phase is different. In Mode III, the sign of the current slope of the other phase is the same. According to magnetic characteristics of the studied SRM, in Modes I and II, the mutual flux introduces ±1% to ±7% incremental-inductance estimation error depending on the phase current and rotor position, while in Mode III, the mutual flux effect does not exist. Therefore, the variable-sampling method is proposed for the outgoing-phase incremental-inductance estimation to ensure that the operation in Mode III is maintained. Due to limitations of the variable-sampling method applied incoming-phase incremental-inductance estimation, the variable-hysteresis-band current controller is proposed for incoming-phase incremental-inductance estimation. With the proposed methods, the mutual flux effect on the incremental-inductance estimation of the SRM can be eliminated. With estimated incremental inductance and measured phase current, the rotor position can be estimated in saturated magnetic region or linear magnetic region. Simulation and experimental results are provided to verify the performance of the proposed rotor position estimation methods working in saturated magnetic region.

II. Dynamic Model of the SRM Considering Mutual Flux and Magnetic Saturation

During commutation, the incoming and outgoing phases are represented as kth and (k–1)th phases, respectively. Phase

Manuscript received June 3, 2014; revised June 27, 2014; accepted July 3, 2014. Date of current version October 7, 2014. This work was supported by the Canada Excellence Research Chairs Program. Recommended for publication by Associate Editor H. Chung.

The authors are with the McMaster Institute for Automotive Research and Technology, McMaster University, Hamilton, ON L8S 4K1 Canada (e-mail: yej25@mcmaster.ca; bilginb@mcmaster.ca; emadi@mcmaster.ca).

Color versions of one or more of the figures in this paper are available online at http://ieeexplore.ieee.org.

Digital Object Identifier 10.1109/TPEL.2014.2337111

voltage equations are derived as follows:

$$v_k = Ri_k + \frac{\partial \lambda_k}{\partial t}$$
$$v_{k-1} = Ri_{k-1} + \frac{\partial \lambda_{k-1}}{\partial t} \quad (1)$$

where v_k, i_k, and λ_k are the phase voltage, current, and flux linkage of *k*th phase, respectively.

The flux linkage can be represented as follows:

$$\begin{bmatrix} \lambda_k \\ \lambda_{k-1} \end{bmatrix} = \begin{bmatrix} L_{k,k} & M_{k,k-1} \\ M_{k-1,k} & L_{k-1,k-1} \end{bmatrix} \begin{bmatrix} i_k \\ i_{k-1} \end{bmatrix} \quad (2)$$

where $\boldsymbol{L}_{k,k}$ and $\boldsymbol{L}_{k-1,k-1}$ are the self-inductances of the *k*th and (*k*–1)th phases, respectively, and $\boldsymbol{M}_{k,k-1}$ and $\boldsymbol{M}_{k-1,k}$ are the mutual inductances.

Considering magnetic saturation, the self-inductance is a function of the rotor position and current. Substituting (2) into (1), the phase voltage equations can be derived as follows:

$$\begin{bmatrix} v_k \\ v_{k-1} \end{bmatrix} = R \begin{bmatrix} i_k \\ i_{k-1} \end{bmatrix} + \begin{bmatrix} L_{\text{inc}\_k} & M_{\text{inc}\_k,k-1} \\ M_{\text{inc}\_k-1,k} & L_{\text{inc}\_k-1,} \end{bmatrix} \begin{bmatrix} \frac{di_k}{dt} \\ \frac{di_{k-1}}{dt} \end{bmatrix} + \omega_m \begin{bmatrix} \frac{\partial L_{k,k}}{\partial \theta} & \frac{\partial M_{k,k-1}}{\partial \theta} \\ \frac{\partial M_{k-1,k}}{\partial \theta} & \frac{\partial L_{k-1,k-1}}{\partial \theta} \end{bmatrix} \begin{bmatrix} i_k \\ i_{k-1} \end{bmatrix} \quad (3)$$

where θ and ω_m are rotor position and angular speed, respectively; incremental inductance and incremental mutual inductance can be denoted as follows:

$$L_{\text{inc}\_k} = L_{k,k} + i_k \frac{dL_{k,k}}{di_k};\ L_{\text{inc}\_k-1} = L_{k-1,k-1} + i_{k-1} \frac{dL_{k-1,k-1}}{di_{k-1}} \quad (4)$$

$$M_{\text{inc}\_k,k-1} = M_{k,k-1} + i_{k-1} \frac{dM_{k,k-1}}{di_{k-1}}. \quad (5)$$

Finite-element analysis (FEA) of the studied motor was conducted using JMAG software [17]. The incremental inductance and mutual inductance are shown in Fig. 1. As shown in Fig. 1(a), incremental inductance is both phase current and rotor position dependent. Therefore, by estimating incremental inductance and measuring the phase current, the rotor position can be estimated by using incremental-inductance-rotor position-current characteristics.

III. Mutual Flux Effect on Inductance Estimation

Phase current is controlled by a hysteresis controller. By considering the mutual flux effect and magnetic saturation, the *k*th phase voltage equation is derived as (6) and (7) when *k*th phase switches are ON and OFF, respectively

$$U_{\text{dc}} = Ri_k + L_{\text{inc}\_k} \frac{di_k(t_{k\_\text{on}})}{dt} + \frac{\partial L_{k,k}}{\partial \theta} i_k \omega_m + M_{\text{inc}\_k,k-1} \frac{di_{k-1}(t_{k\_\text{on}})}{dt} + \frac{\partial M_{k,k-1}}{\partial \theta} i_{k-1} \omega_m \quad (6)$$

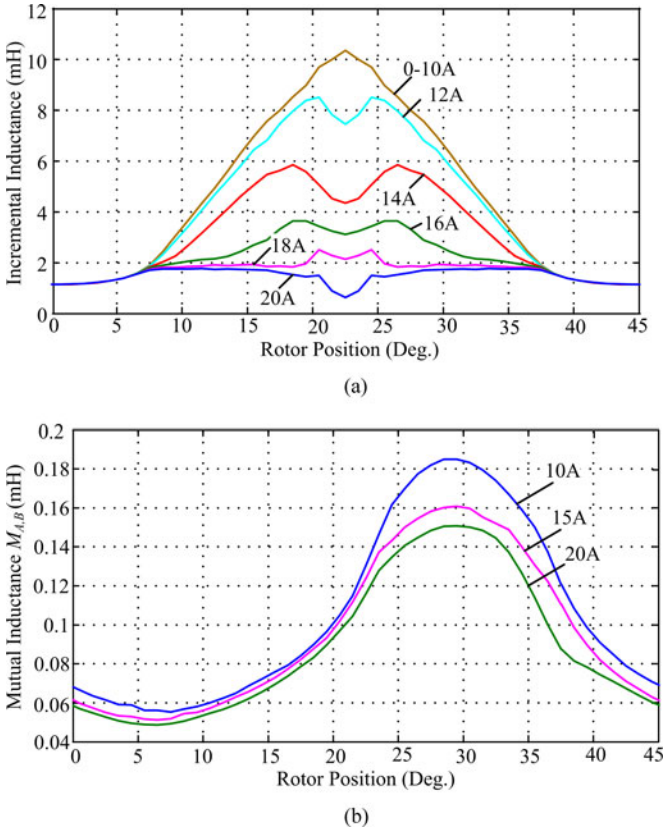

Fig. 1. FEA inductance profiles of 12/8 SRM.

$$-U_{\text{dc}} = Ri_k + L_{\text{inc}\_k} \frac{di_k(t_{k\_\text{off}})}{dt} + \frac{\partial L_{k,k}}{\partial \theta} i_k \omega_m + M_{\text{inc}\_k,k-1} \frac{di_{k-1}(t_{k\_\text{off}})}{dt} + \frac{\partial M_{k,k-1}}{\partial \theta} i_{k-1} \omega_m \quad (7)$$

where t_{k_on} and t_{k_off} are time instants when the *k*th phase switches are ON and OFF, respectively, $di_{k(t_{k\_\text{on}})}/dt$ and $di_k(t_{k\_\text{off}})/dt$ are the *k*th phase current slopes at t_{k_on} and t_{k_off}, respectively, and U_{dc} is the dc-link voltage.

The switching period is short enough, and therefore, the variation of the mechanical speed, inductance, back electromotive force, and resistance can be neglected. Subtracting (6) by (7), the *k*th phase incremental inductance can be estimated as (8) by considering the mutual inductance and magnetic saturation

$$L_{\text{inc}\_k\_m} = \frac{2U_{\text{dc}} - M_{\text{inc}\_k,k-1} \left(\frac{di_{k-1}(t_{k\_\text{on}})}{dt} - \frac{di_{k-1}(t_{k\_\text{off}})}{dt} \right)}{\frac{di_k(t_{k\_\text{on}})}{dt} - \frac{di_k(t_{k\_\text{off}})}{dt}}. \quad (8)$$

If the mutual inductance is neglected, incremental inductance can be estimated as follows:

$$L_{\text{inc}\_k} = \frac{2U_{\text{dc}}}{\frac{di_k(t_{k\_\text{on}})}{dt} - \frac{di_k(t_{k\_\text{off}})}{dt}}. \quad (9)$$

Therefore, incremental-inductance estimation error due to mutual flux can be derived as follows:

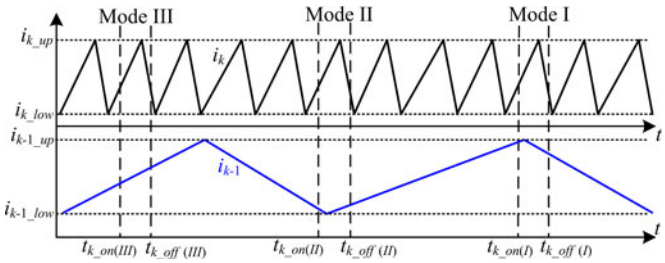

Fig. 2. Illustration of three modes during kth phase inductance estimation.

$$err_k = (L_{\mathrm{inc}\_k\_m} - L_{\mathrm{inc}\_k})/L_{\mathrm{inc}\_k\_m} = \frac{-M_{\mathrm{inc}\_k,k-1}\left(\frac{di_{k-1}(t_{k\_\mathrm{on}})}{dt} - \frac{di_{k-1}(t_{k\_\mathrm{off}})}{dt}\right)}{2U_{\mathrm{dc}} - M_{\mathrm{inc}\_k,k-1}\left(\frac{di_{k-1}(t_{k\_\mathrm{on}})}{dt} - \frac{di_{k-1}(t_{k\_\mathrm{off}})}{dt}\right)}. \quad (10)$$

In order to analyze the incremental-inductance estimation error due to the mutual flux, three modes are defined during kth phase incremental-inductance estimation as shown in Fig. 2: Modes I–III. Since the incremental inductance of the incoming phase (kth phase) is much lower, kth phase current slope is much higher than (k–1)th phase. Upper and lower current references of kth phase are denoted as i_{k_up} and i_{k_low}, respectively, and upper and lower current references of (k–1)th phase are denoted as i_{k-1_up} and i_{k-1_low}, respectively. The positive-current slope and negative-current slope of kth phase are sampled at $t_{k\_\mathrm{on(III)}}$ and $t_{k\_\mathrm{off(III)}}$ in Mode III, $t\_k_{\mathrm{on(II)}}$ and $t\_k_{\mathrm{on(II)}}$ in Mode II, and $t\_k_{\mathrm{on(I)}}$ and $t_{k\_\mathrm{off(I)}}$ in Mode I, respectively.

By considering the magnetic saturation, the incremental-inductance estimation error due to the mutual flux can be derived as (11) and (12), shown at the bottom of the page, in Modes I and II, respectively [16]. In Mode III, at $t_{k\_\mathrm{on(III)}}$ and $t_{k\_\mathrm{off(III)}}$, (k–1)th phase current slope has the same sign (either both negative or positive). Therefore, the mutual flux effect does not exist in Mode III

Comparing (11) and (12), the absolute value of incremental-inductance estimation error in Mode I is slightly higher than that in Mode II. Based on the magnetic characteristics of the studied SRM shown in Fig. 1, the absolute value of incremental-inductance estimation error of phase A due to mutual flux from phase C in Mode I is shown in Fig. 3. Considering the magnetic saturation, incremental-inductance estimation error due to mutual flux is both rotor position and current dependent. As shown in Fig. 4, the mutual flux from phase C introduces around maximum 7% and minimum 1% error in phase A incremental-inductance estimation.

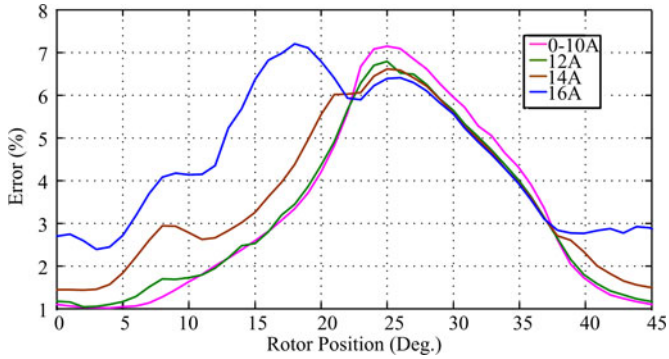

Fig. 3. Incremental-inductance estimation error of phase A due to mutual flux.

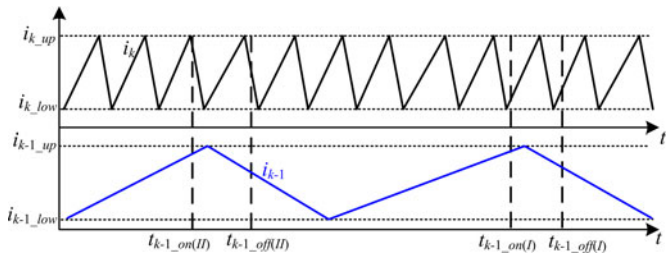

Fig. 4. Illustration of incremental-inductance estimation of (k–1)th phase using the proposed variable-sampling scheme.

IV. Proposed Methods to Eliminate Mutual Flux Effect

Based on the error analysis in the last section, the mutual flux introduces a maximum ±7% incremental-inductance estimation error in Modes I and II, while the mutual flux effect does not exist in Mode III. Two methods will be proposed, which forces the incremental-inductance estimation to operate in Mode III exclusively: the variable-sampling method for the outgoing phase and variable-hysteresis-band current control for the incoming phase.

A. Proposed Variable-Sampling Scheme for Outgoing-Phase Incremental-Inductance Estimation

Illustration of the variable-sampling scheme for (k–1)th phase (outgoing phase) is shown in Fig. 4. The positive phase current slope of (k–1)th phase is sampled at time instants $t_{k-1(\mathrm{I})\_\mathrm{on}}$ and $t_{k-1(\mathrm{II})\_\mathrm{on}}$, which are fixed. During commutation, the sign of kth phase current slope is changed several times during (k–1)th phase self-inductance estimation. Therefore, in Mode I or II, the (k–1)th phase negative-phase-current-slope sampling point $t_{k-1(\mathrm{I})\_\mathrm{off}}$ can be adjusted to ensure kth phase current slope at $t_{k-1(\mathrm{I})\_\mathrm{off}}$ and $t_{k-1(\mathrm{I})\_\mathrm{on}}$ have the same signs. Therefore,

$$err_{k(\mathrm{I})} = \frac{-M_{\mathrm{inc}\_k,k-1}}{L_{\mathrm{inc}\_k-1} + M_{\mathrm{inc}\_k,k-1}\frac{(L_{\mathrm{inc}\_k-1} - M_{\mathrm{inc}\_k,k-1})}{(L_{\mathrm{inc}\_k} - M_{\mathrm{inc}\_k,k-1})} - M_{\mathrm{inc}\_k,k-1}} \quad (11)$$

$$err_{k(\mathrm{II})} = \frac{M_{\mathrm{inc}\_k,k-1}}{L_{\mathrm{inc}\_k-1} + M_{\mathrm{inc}\_k,k-1}\frac{L_{\mathrm{inc}\_k-1} + M_{\mathrm{inc}\_k,k-1}}{L_{\mathrm{inc}\_k} - M_{\mathrm{inc}\_k,k-1}} + M_{\mathrm{inc}\_k,k-1}} \quad (12)$$

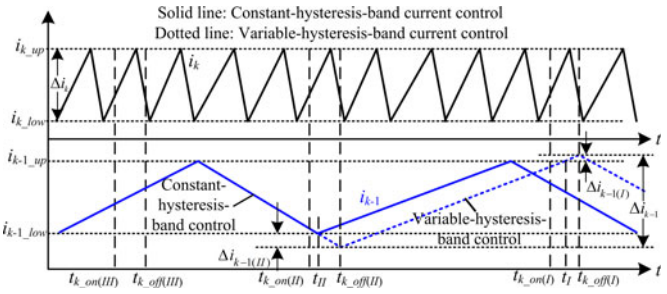

Fig. 5. Illustration of the proposed variable-hysteresis-band current controller.

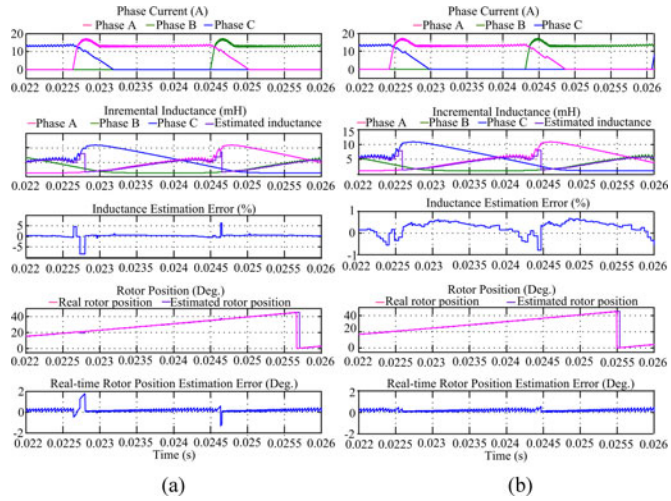

Fig. 6. Simulation results of rotor position estimation ($T_{\rm ref} = 3$ N · m, Speed $= 1500$ r/min). (a) Rotor position estimation method without variable hysteresis band and sampling. (b) Proposed rotor position estimation.

the outgoing-phase incremental-inductance estimation is always operating in Mode III by using this scheme. Since the phase current slope of *k*th phase (incoming phase) is much higher than (*k*–1)th phase, the sign of (*k*–1)th phase current slope is changed only once or not changed at all. Therefore, the variable-sampling scheme cannot be applied to the incoming-phase incremental-inductance estimation.

B. Proposed Variable-Hysteresis-Band Current Control for Incoming-Phase Incremental-Inductance Estimation

Fig. 5 illustrates the principle of the proposed variable-hysteresis-band current control during the *k*th phase estimation.

The basic concept of the variable-hysteresis-band current control method is to make sure that the switching state of (*k*–1)th phase is unchanged during the time intervals $t_{k\_{\rm on(II)}}$-$t_{k\_{\rm off(II)}}$ and $t_{k\_{\rm on(I)}}$-$t_{k\_{\rm off(I)}}$. Therefore, the sign of (*k*–1)th phase current slope is unchanged in these intervals. When the incremental-inductance estimation of *k*th phase is completed at $t_{k_{\rm on(II)}}$ and $t_{k_{\rm off(I)}}$, switches of (*k*–1)th phase are turned off or on according to the error between (*k*–1)th phase current and its reference. Since the sign of (*k*–1)th phase current remains unchanged during the sampling interval, the *k*th phase incremental-inductance estimation is working in Mode III exclusively.

V. Simulation Verification

With the estimated incremental-inductance and measured phase current, the rotor position can be obtained. The proposed position estimation method is compared to the method without variable hysteresis band and variable sampling by simulations. Linear torque sharing function [18] is used to generate the current reference. Turn-on angle $\theta_{\rm on}$, turn-off angle $\theta_{\rm off}$, and overlapping angle θ_{ov} of linear TSF are set to 5°, 20°, and 2.5°, respectively. DC-link voltage is 300 V. The sampling time $t_{\rm sample}$ is set to 5 μs and current hysteresis band is set to 0.5 A. The incremental-inductance estimation error and rotor position estimation error are denoted as

$$err_L = \frac{L_{\rm real} - L_e}{L_{\rm real}};\ err_\theta = \theta_{\rm real} - \theta_e \tag{13}$$

where $L_{\rm real}$ and L_e are real and estimated inductance, respectively, and $\theta_{\rm real}$ and θ_e are real position and estimated position, respectively.

The torque reference is set to 3 N · m. Fig. 6 shows simulation results of the proposed rotor position estimation with and without variable hysteresis band and sampling at 1500 r/min.

As shown in Fig. 6, due to magnetic saturation, incremental inductance varies with rotor position and phase current. Since phase current is not constant, the SRM is operating either in saturated magnetic region or linear magnetic region. Therefore, both incremental inductance and phase current are necessary for estimating the rotor position. The maximum incremental-inductance estimation error without variable hysteresis band and sampling is $\pm 7\%$, which matches theoretical analysis given in Fig. 4. Due to incremental-inductance estimation error, the maximum real-time rotor position estimation error is around $\pm 2.0°$. By using the proposed variable-hysteresis-band current controller and variable-sampling self-inductance estimation, the maximum inductance estimation error is decreased to $\pm 0.7\%$. As a result, the maximum real-time rotor position estimation error are decreased to $+0.5°$. Therefore, the proposed rotor position estimation method demonstrates around 2° accuracy improvement by eliminating the mutual flux effect on rotor position estimation of the SRM.

VI. Experimental Verification

The proposed variable-hysteresis-band current control and variable-sampling position estimation methods are compared to the position estimation methods without variable hysteresis band and sampling experimentally on a 2.3 kW, 6000 r/min, three-phase 12/8 SRM. Current hysteresis band is set to 0.5 A and dc-link voltage is set to 300 V. Field-programmable gate array EP3C25Q240 is used for digital implementation of the rotor position estimation methods.

The torque reference is set to 3 N · m and the speed is 1500 r/min. From the experimental results shown in Fig. 7, it can be noticed that real-time rotor position estimation error has positive bias. This is because the selected digital-to-analog

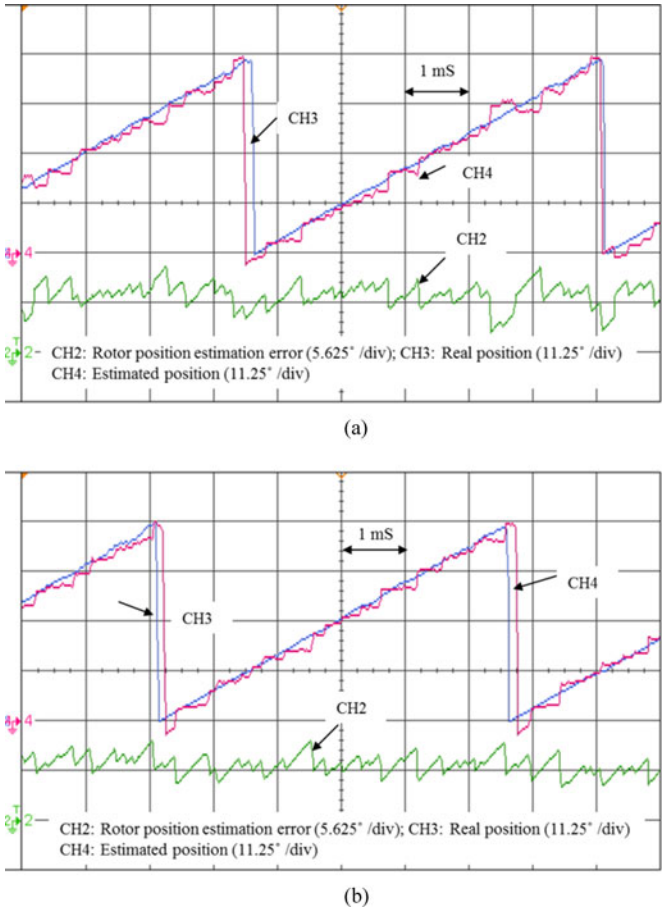

Fig. 7. Experimental result of rotor position estimation at 1500 r/min ($T_{\mathrm{ref}} = 3\ \mathrm{N} \cdot \mathrm{m}$). (a) Rotor position estimation without variable hysteresis band and sampling. (b) Proposed rotor position estimation.

conversion chip is unipolar. Therefore, 5.625° offset is added to position error in the next a couple of figures. The real-time position estimation error without variable hysteresis band and sampling is $+4.6°$ and $-3.4°$. By using the proposed method, the real-time rotor position estimation error of the proposed method is decreased to $+3.3°$ and $-1.3°$. Due to the noise and quantization error in the current sensing, phase current slope sensing error is higher, leading to the increase in the real-time rotor position estimation error compared with simulation results. However, the proposed method still shows an increase of approximately 2° in position estimation accuracy.

VII. Conclusion

In this letter, two methods are proposed to eliminate the mutual flux effect on rotor position estimation of SRM drives operating at both linear and saturated magnetic regions without *a priori* knowledge of mutual flux. The mutual flux theoretically introduces $\pm 1\%$ to $\pm 7\%$ incremental-inductance estimation error, which is both phase current and rotor position dependent. However, the mutual flux effect on incremental-inductance estimation can be eliminated by using the proposed two methods: one is the variable-sampling method for the outgoing phase and the other is variable-hysteresis-band current control for the incoming phase. With accurately estimated incremental inductance and measured phase current, rotor position can be better estimated. The proposed method is verified by both simulation and experimental results with a 2.3 kW, 6000 r/min, three-phase 12/8 SRM. Both simulation results and experimental results show that the proposed method improves around 2° rotor position estimation accuracy compared with the methods neglecting the mutual flux.

References

[1] M. Krishnamurthy, C. C. Edrington, and B. Fahimi, "Prediction of rotor position at standstill and rotating shaft conditions in switched reluctance machines," *IEEE Trans. Power Electron.*, vol. 21, no. 1, pp. 225–233, Jan. 2006.

[2] L. Shen, J. H. Wu, and S. Y. Yang, "Initial position estimation in SRM using bootstrap circuit without predefined inductance parameters," *IEEE Trans. Power Electron.*, vol. 26, no. 9, pp. 2449–2456, Sep. 2011.

[3] C. J. Bateman, B. C. Mecro, A. C. Clothier, P. P. Acarnley, and N. D. Tuftnell, "Sensorless operation of an ultra-high speed switched reluctance machine," *IEEE Trans. Ind. Appl.*, vol. 46, no. 6, pp. 2329–2337, Nov./Dec. 2010.

[4] K. R. Geldhof, A. P. M. Van den Bossche, and J. A. Melkebeek, "Rotor-position estimation of switched reluctance motors based on damped voltage resonance," *IEEE Trans. Ind. Electron.*, vol. 57, no. 9, pp. 2954–2960, Sep. 2010.

[5] G. Pasquesoone, R. Mikail, and I. Husain, "Three-phase switched reluctance machines using pulse injection and two thresholds," *IEEE Trans. Ind. Appl.*, vol. 47, no. 4, pp. 1724–1731, Jul./Aug. 2013.

[6] B. Fahimi, A. Emadi, and R. B. Sepe, "Four quadrant position sensorless control in SRM drives over the entire speed range," *IEEE Trans. Power Electron.*, vol. 20, no. 1, pp. 154–163, Jan. 2005.

[7] J. Cai and Z. Deng, "Sensorless control of switched reluctance motor based on phase inductance vectors," *IEEE Trans. Power Electron.*, vol. 27, no. 7, pp. 3410–3423, Jul. 2012.

[8] L. Shen, J. H. Wu, and S. Y. Yang, "Initial position estimation in SRM using bootstrap circuit without predefined inductance parameters," *IEEE Trans. Power Electron.*, vol. 26, no. 9, pp. 2449–2456, Sep. 2011.

[9] I. H. Al-Bahadly, "Examination of a sensorless rotor position measurement method for switched reluctance drive," *IEEE Trans. Ind. Electron.*, vol. 55, no. 1, pp. 288–295, Jan. 2008.

[10] K. Ha, R. Kim, and R. Krishnan, "Position estimation in switched reluctance motor drives using the first switching harmonics through Fourier series," *IEEE Trans. Ind. Electron.*, vol. 58, no. 12, pp. 5352–5359, Dec. 2012.

[11] G. J. Li, S. Hliout, E. Hoang, M. Gabsi, and C. Bacpe, "Comparative study of switched reluctance motors performances for two current distributions and excitation modes," in *Proc. IEEE Conf. Ind. Electron.*, Porto, Portugal, Nov. 2009, pp. 4047–4052.

[12] A. Jin-Woo, O. Seok-Gyu, M. Jae-Won, and H. Young-Moon, "A three-phase switched reluctance motor with two-phase excitation," *IEEE Trans. Ind. Appl.*, vol. 35, no. 5, pp. 1067–1075, Sep./Oct. 1999.

[13] C. S. Edrington, B. Fahimi, and M. Krishnamurthy, "An autocalibrating inductance model for switched reluctance motor drives," *IEEE Trans. Ind. Electron.*, vol. 54, no. 4, pp. 2165–2173, Aug. 2007.

[14] D. Panda and V. Ramanarayanan, "Mutual flux and its effect on steady-state performance and position estimation of even and odd number phases witched reluctance motor drive," *IEEE Trans. Magn.*, vol. 43, no. 8, pp. 3445–3456, Aug. 2007.

[15] I. S. Manolas, A. G. Kladas, and S. N. Manias, "Finite-element-based estimator for high-performance switched reluctance machine drives," *IEEE Trans. Magn.*, vol. 45, no. 3, pp. 1266–1369, Mar. 2009.

[16] J. Ye, B. Bilgin, and A. Emadi, "Elimination of mutual flux effect on rotor position estimation of switched reluctance motor drives," *IEEE Trans. Power Electron.*, to be published.

[17] *JMAG. Application Note*, JSOL Corporation, Tokyo, Japan, 2013. [Online]. Available: http://www.jmag-international.com/.

[18] X. D. Xue, K. W. E. Cheng, and S. L. Ho, "Optimization and evaluation of torque sharing function for torque ripple minimization in switched reluctance motor drives," *IEEE Trans. Power Electron.*, vol. 24, no. 9, pp. 2076–2090, Sep. 2009.